

Efficient Cross-View Localization in 6G Space-Air-Ground Integrated Network

Min Hao, Yanbing Xu, Maoqiang Wu, Jinglin Huang, Chen Shang, Jiacheng Wang, Ruichen Zhang, Jiawen Kang, Dusit Niyato, *Fellow, IEEE*, Zhu Han, *Fellow, IEEE* and Wei Ni, *Fellow, IEEE*

Abstract—Recently, visual localization has become an important supplement to improve localization reliability, and cross-view approaches can greatly enhance coverage and adaptability. Meanwhile, future 6G will enable a globally covered mobile communication system, with a space-air-ground integrated network (SAGIN) serving as key supporting architecture. Inspired by this, we explore an integration of cross-view localization (CVL) with 6G SAGIN, thereby enhancing its performance in latency, energy consumption, and privacy protection. First, we provide a comprehensive review of CVL and SAGIN, highlighting their capabilities, integration opportunities, and potential applications. Benefiting from the fast and extensive image collection and transmission capabilities of the 6G SAGIN architecture, CVL achieves higher localization accuracy and faster processing speed. Then, we propose a split-inference framework for implementing CVL, which fully leverages the distributed communication and computing resources of the 6G SAGIN architecture. Subsequently, we conduct joint optimization of communication, computation, and confidentiality within the proposed split-inference framework, aiming to provide a paradigm and a direction for making CVL efficient. Experimental results validate the effectiveness of the proposed framework and provide solutions to the optimization problem. Finally, we discuss potential research directions for 6G SAGIN-enabled CVL.

Index Terms—Cross-view, 6G, SAGIN, split-inference.

I. INTRODUCTION

Vision-based localization is a key enabling technology for achieving high-precision and low-latency spatial awareness in 6G networks. In fields such as autonomous vehicles, unmanned aerial vehicles (UAVs), and augmented reality (AR), vision-based localization utilizes image or video information to determine the position and orientation of targets and has been widely adopted [1]. In particular, in scenarios with weak satellite signals, such as urban canyons, indoor environments, and low-altitude UAV operations, vision-based localization offers significant advantages over traditional global navigation satellite system (GNSS)- or inertial measurement unit (IMU)-based methods. Despite significant progress in vision-based localization, existing methods largely rely on images captured from similar viewpoints and scales, which is insufficient to meet the intelligent, immersive, and high-precision localization requirements envisioned for 6G applications.

To overcome the limitations of same-view localization, cross-view localization (CVL) has emerged as a promising paradigm [2]. CVL enables feature matching between a given query image and a reference image database captured from different viewpoints or altitudes, through which the absolute position and orientation of the query image can be estimated. A comparison of the advantages and limitations between CVL

and same-view localization is presented in Table I. CVL is capable of supporting multi-scale and multi-view localization, and enhances robustness to diverse scenarios. However, large cross-domain heterogeneity remains a major challenge for CVL. Significant differences in viewpoint, resolution, and imaging modalities across space, air, and ground visual data make feature matching highly challenging. Moreover, CVL suffers from privacy leakage, insufficient computational power, and high latency when processing multi-source data [3].

Motivated by the potential benefits of 6G, this article investigates CVL in the context of 6G space-air-ground integrated networks (SAGIN). The SAGIN is constructed by integrating satellite communications, high-altitude platforms, and terrestrial networks, thereby enabling global coverage, seamless connectivity, and low-latency ubiquitous communication infrastructure [4]. Using CVL in 6G SAGIN brings several notable advantages. Although GNSS signals may be unreliable in complex environments, fusing multi-view information significantly improves localization reliability and robustness, thus making the system more resilient to occlusion and environmental changes. Moreover, combining global references from aerial and satellite imagery with local details from ground-level images can enhance the positioning accuracy, thereby achieving meter or even sub-meter level precision in urban scenarios. In addition, CVL can perform forward feature extraction at edge nodes within 6G SAGIN, requiring only the transmission of low-dimensional features and thus reducing communication overhead. Finally, 6G SAGIN inherently possess distributed computing and communication capabilities, making them inherently compatible with the hierarchical processing of CVL [5].

To achieve the above-mentioned objectives of CVL, this study proposes the architecture of CVL with cross-domain feature alignment, edge collaborative computing, and privacy preservation. We develop a space-air-ground split-inference framework to enable image feature matching, while addressing the trade-off among privacy protection, energy consumption, and latency. The main contributions are summarized as follows:

- We present an overall perspective and architecture that integrates 6G SAGIN with CVL. Building on this foundation, we introduce important research directions for CVL within SAGIN, including communication optimization, privacy preservation, and visual processing.
- We propose a space-air-ground collaborative split-inference framework, where multi-view image features are extracted and matched via terrestrial base stations.

TABLE I: Comparison of Visual Data Sources and Cross-Domain Fusion for Localization

Dimension	Satellite Images	UAV Images	Ground Images	Tri-fusion (Cross-View Loc.)
Viewpoint	Nadir (vertical)	Top-down + oblique	Horizontal / first-person	Multi-view fusion
Resolution	Meter-level	Centimeter-level	Sub-meter or finer	Cross-scale integration
Dynamics	Static	Highly dynamic	Moderately dynamic	Multi-dynamic adaptation
Coverage	10 km	≤ 1 km	Local area	Global-to-local coverage
Advantages	Wide-area positioning	High resolution; flexible	Rich fine-grained details	High precision; robustness
Limitations	Refresh slowly	Unstable features	Severe occlusion	Large cross-domain heterogeneity
Applications	Digital twins	UAV inspection; low-altitude economy	V2X / connected vehicles; AR nav.	Autonomous driving; 6G

The framework also addresses the joint optimization of privacy preservation, energy consumption, and latency.

- We evaluate the proposed framework through a case study, in which experiments with varying image quantities and different types of privacy attacks demonstrate that the framework effectively improves localization accuracy and enhances data security.

The rest of the article is organized as follows: An overview of CVL and 6G SAGINs is presented in Section II. Section III describes the proposed split-inference framework and optimization scheme, while Section IV presents the experimental evaluation of the proposed methods. We discuss future research directions in Section V. Finally, we conclude our article in Section VI.

II. OVERVIEW OF CROSS-VIEW LOCALIZATION AND SAGIN

A. Cross-View Localization

CVL is an emerging technique that estimates the absolute position and orientation of a query image by matching it with reference images captured from different viewpoints, altitudes, or modalities [6]. As shown in Fig. 1, CVL leverages heterogeneous visual data sources within space-air-ground domains to achieve precise localization, particularly in scenarios where accurate GNSS signals cannot be received due to building obstructions or natural disasters. CVL typically involves three main stages:

- **Feature Extraction:** Local or global features are extracted from both query and reference images using traditional descriptors or deep learning-based models.
- **Feature Matching:** Extracted features are aligned across multi-view or cross-modal datasets to establish visual correspondences, often enhanced through semantic cues or multi-modal fusion.
- **Localization:** The absolute position is determined by either assigning the geographic coordinates of the best-matching reference image or performing geometric transformations for relative pose estimation. Alternatively, end-to-end localization models can be directly designed and trained, where the input is an image and the output is the estimated location.

Feature extraction is a critical step in CVL, and different studies define features in different ways, which can be broadly categorized as follows:

- **Image-feature-based methods:** The core idea is to extract local or global features from images and identify corresponding points across cross-domain data. Representative methods include scale-invariant feature transform (SIFT), oriented fast and rotated brief (ORB), and network vector of locally aggregated descriptors (NetVLAD) [7]. These methods are theoretically well-established and provide strong algorithmic interpretability. However, their localization accuracy is low when dealing with large viewpoint variations or substantial differences in resolution.
- **Semantic-feature-based methods:** With the advancement of artificial intelligence, the semantic information of images has attracted increasing attention. The core idea is to leverage deep learning to extract cross-view-invariant semantic features, enabling matching and localization. Adaptability to cross-view and cross-scale variations is one of their main advantages. However, the models heavily depend on large volumes of labeled data. Representative methods include convolutional neural network (CNN), residual network (ResNet), and Vision Transformer [8].
- **Multi-modal feature fusion-based methods:** CVL can also be realized by incorporating information from other modalities. The core mechanism is to integrate multi-source data such as visual, light detection and ranging (LiDAR), IMU, and GNSS for localization. These methods enable the joint extraction of semantic and geometric features, offering high robustness. However, the overall system complexity increases, necessitating latency optimization. Existing methods include contrastive language-image pre-training (CLIP), local feature transformer (LoFTR), and self-distillation with no labels v2 (DINOv2) [9].

From the characteristics of the aforementioned methods, the core features of CVL can be identified as cross-domain fusion, high-accuracy robustness, and native adaptability to 6G. CVL not only enables matching among high-altitude satellite images, low-altitude UAV images, and ground-level vehicle-view images, but also supports correspondence across

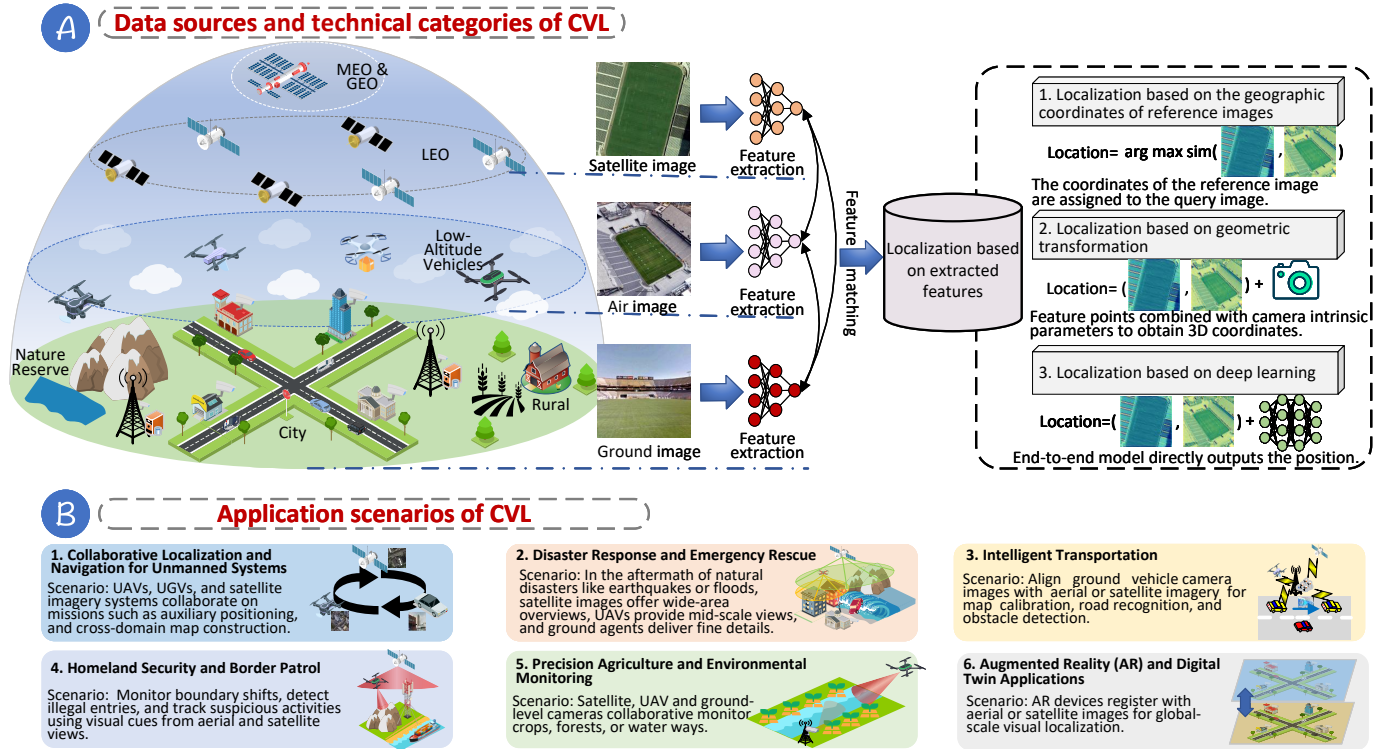


Fig. 1: Overview of Cross-View Localization. illustrates the data sources and localization methods of CVL. 6G SAGIN provides multi-source image data for CVL, which enables localization through different methods. *Part B* presents the application scenarios of CVL from different perspectives.

nadir, oblique, and horizontal view images. In the scenarios where GNSS signals are weak or unavailable, CVL can still perform reliable localization and leverage multi-view data to compensate for the degradation in localization accuracy due to low image resolution. Meanwhile, CVL is inherently well-suited to high-bandwidth, low-latency, and multi-modal big data scenarios. Based on the above characteristics, Fig. 1 illustrates the potential application scenarios of CVL.

B. 6G Space-Air-Ground Integrated Networks

SAGIN unifies high-altitude platforms (satellites), low-altitude platforms (UAVs or balloons), and ground platforms (cellular networks) into a single 6G network. The 6G SAGIN aims to achieve global coverage, ubiquitous connectivity, ultra-reliability with low latency, integrated sensing and communication, and sustainability [10], [11].

There are numerous application scenarios for 6G SAGIN, and an example is illustrated using a UAV-based urban delivery system. In the low-altitude economy, UAVs are expected to undertake tasks such as parcel delivery, emergency supply transportation, and urban infrastructure inspection. By contrast, UAVs operating in urban canyon environments face challenges such as GNSS signal outages and communication interruptions [12]. 6G SAGIN addresses these challenges by integrating satellites (Space), high-altitude platforms (Air), and terrestrial networks (Ground) as follows:

- Before flight, UAVs interact with the air traffic management system to download 3D flight routes based

on the urban digital twin. A SAGIN allocates multi-domain resources to ensure prioritized availability of communication links.

- During flight, the UAVs continuously receive signals from low earth orbit (LEO) satellites, high-altitude relay platforms, and ground roadside units (RSUs). When entering densely built-up areas, CVL is activated, allowing the UAVs to share point cloud and visual data with the RSUs to achieve sub-meter-level obstacle avoidance.
- After completing the flight, the UAVs upload their flight paths, communication logs, and energy consumption data to the urban digital twin, enabling subsequent simulation and optimization.

C. Summary

CVL is a typical application scenario of SAGIN, while SAGIN provides the optimal infrastructure for CVL. The two mutually complement each other, jointly driving the deployment of 6G in the low-altitude economy, intelligent transportation, emergency rescue, and national defence security. Based on overview of the CVL and 6G SAGIN, we highlight the following critical insights.

- **CVL needs to be seamless integrated with 6G SAGIN.** CVL has a wide range of applications and requires diverse types of imagery. 6G SAGIN features global coverage, low latency, high bandwidth, and AI-native capabilities, which precisely meet the CVL requirements for real-time acquisition of cross-domain multi-source visual data and enable real-time cross-view visual matching.

- **A more efficient distributed framework framework is required to realize CVL.** Real-time images are stored across various space-air-ground devices. However, device heterogeneity causes traditional CVL methods to rely heavily on offline image databases and local feature matching, resulting in significant challenges in terms of accuracy, real-time performance, and scalability.
- **Joint optimization of communication, computation, and privacy is required in CVL.** While 6G networks provide a powerful infrastructure for CVL, massive data transmission and intensive computational overhead still pose significant challenges to user experience. Furthermore, images collected by various devices may contain sensitive information such as residences, vehicles, and faces, and cross-domain sharing substantially increases privacy risks.

III. SAGIN-ENABLED CROSS-VIEW LOCALIZATION

A. Requirement

Achieving high-quality CVL requires robust communication infrastructure, and CVL should be natively embedded within 6G networks so that its implementation is tightly integrated with the network architecture. Within the communication and computation architecture of 6G networks, CVL can be optimized from the following aspects:

- **Architecture Alignment:** 6G emphasizes a fully integrated, ubiquitous, and intelligent network architecture spanning space, air, ground, and sea. The research direction of CVL should align with this development trend by pursuing higher localization accuracy and adopting more reliable methods to seamlessly integrate into the 6G network ecosystem.
- **Distributed Inference:** To improve efficiency, 6G will be developed based on a fully distributed infrastructure that integrates communication, computation, sensing, and storage, and the implementation of CVL will likewise be distributed. Splitting feature-matching models for distributed training and inference is a key approach to enhancing the efficiency of CVL.
- **Quality of service optimization:** As an important task within 6G networks, CVL requires further optimization of its quality of service (QoS). In particular, when using split-inference for feature matching, the communication latency, computational energy consumption, and privacy cost across space-air-ground devices need to be jointly optimized.

B. Proposed Framework

We propose a split-inference framework to enhance the adaptability of CVL in 6G SAGIN, along with a joint optimization scheme for communication, computation, and confidentiality (Tri-Co) within the framework.

1) *CVL based on Split-Inference:* Split-inference is an AI model deployment technique in which a neural network is divided into two (or more) parts and executed across different devices. Typically, the front part of the model runs on a

resource-constrained edge device (e.g., UAVs, vehicles, or satellites) to extract intermediate features, while the remaining part runs on a more powerful edge server or cloud server [13]. Split-inference has many practical applications, such as UAVs used for search and rescue in disaster areas with limited communication capabilities. UAVs equipped with cameras or sensors can execute the early layers of a computer vision model to extract features locally, and then transmit these features to an edge server or ground station for higher-level inference tasks such as object recognition and tracking. Part (a) of Fig. 2 illustrates the CVL process based on split-inference.

The image data in Fig. 2 are sourced from satellites, UAVs, and vehicles across the space-air-ground domains. Satellite images serve as reference images, from which features are extracted and associated with corresponding geographic coordinate tags. The features of satellite images and their associated tags are pre-stored in vector form on a ground server, and organized into a database to facilitate on-demand retrieval for CVL tasks. Images captured by UAVs and vehicles can both serve as query images for CVL. Alternatively, any of them can be used as a reference image while the rest functions as a query image. The acquisition cost of satellite imagery is relatively high, whereas the imaging cost of air and ground devices is much lower. Therefore, CVL can achieve localization by selecting a single satellite image together with multiple images captured within the Earth's lower atmosphere and surface.

The feature extraction models for satellite-view, UAV-view, and vehicle-view images are implemented as three neural networks with identical architectures but different parameters (e.g., CNN or Transformer). During model training, each location is treated as a distinct class, and the outputs of the three neural networks are then fed into a shared linear classifier. This constrains images from different viewpoints to the same discriminative space, thereby achieving cross-view alignment. During model inference, the feature extraction model for satellite images is executed on servers aboard LEO satellites. This allows the extracted feature data to be transmitted instead of the raw images, thereby reducing communication costs. The feature extraction models for UAVs and vehicles are divided into two parts: the front part is executed on the terminal devices (UAVs and vehicles), while the back part runs on a ground base station. This design conserves the computational resources of UAVs and vehicles, thereby reducing both computational and communication energy consumption. Moreover, since images captured by UAVs and vehicles may involve sensitive information such as faces, license plates, and restricted areas, transmitting intermediate feature data can effectively mitigate privacy leakage risks.

After feature extraction, the features from the three types of images are jointly matched. The servers connected to ground base stations obtain features from images of different viewpoints and perform nearest-neighbour retrieval using cosine similarity, where a similarity greater than a predefined threshold is regarded as a successful match. Once feature matching is successfully achieved, the query images can be localized by assigning them the geographic coordinates of the corresponding reference images. The above framework is broadly applicable to CVL tasks within 6G SAGIN, while

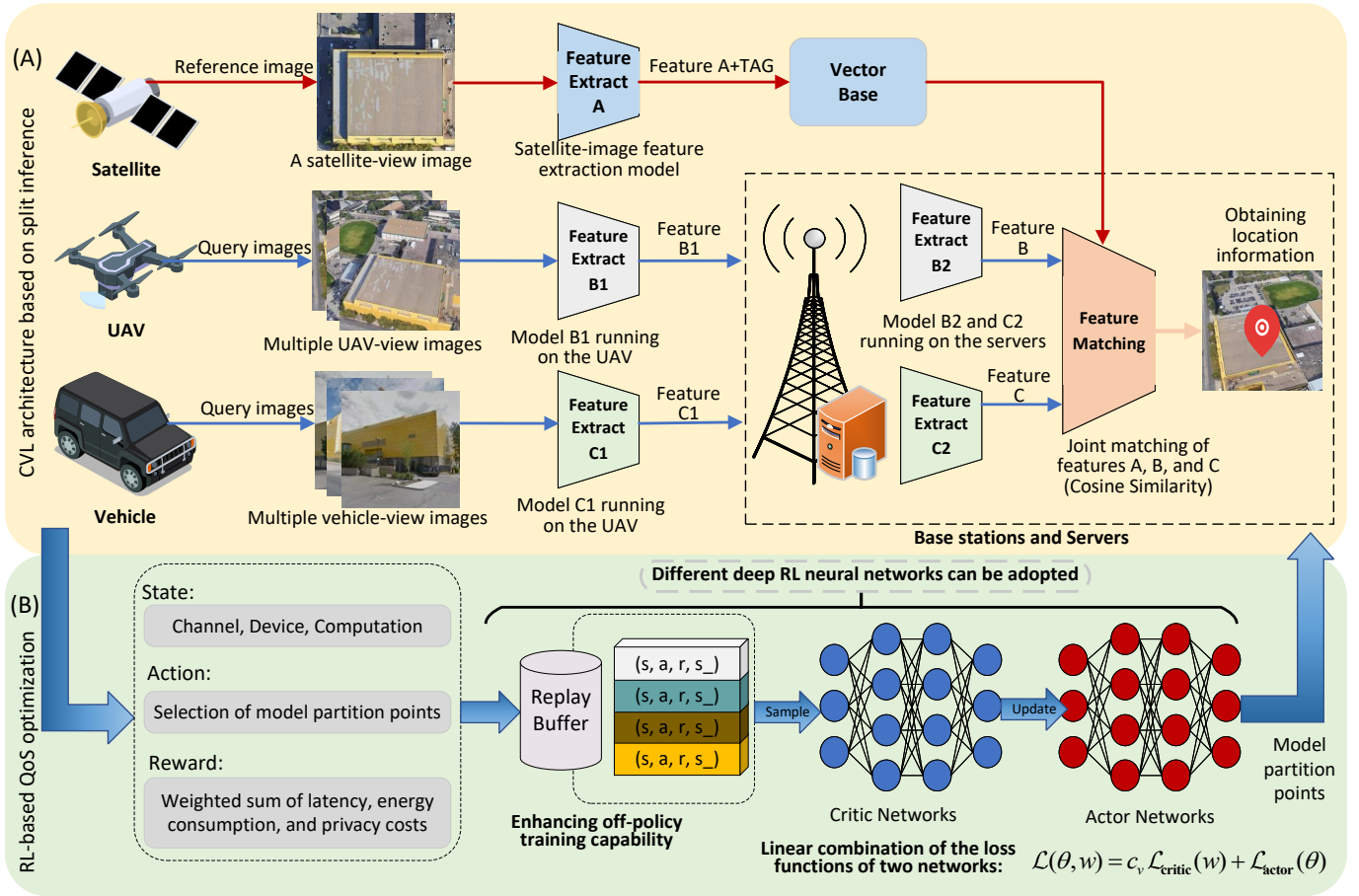


Fig. 2: Split-inference framework for CVL in 6G SAGIN. *Part A* illustrates the process of implementing CVL through split-inference within the 6G SAGIN. *Part B* presents the Tri-Co optimization scheme based on reinforcement learning.

also accounting for limited device computing capabilities and ensuring the protection of sensitive data.

2) *Tri-Co-Optimization Scheme*: In the above framework, to achieve a better user experience, joint optimization across communication, computation, and confidentiality is required.

- **Communication**: The communication links for collecting multi-source images required by CVL are long distance and highly heterogeneous. Various types of image data must be transmitted among satellites, UAVs, ground devices, and a cloud server, where even slight data redundancy can result in network congestion. In split-inference, the selection of model partition points determines the size of intermediate features, which in turn affects the latency and energy consumption during transmission. Additionally, for UAVs and vehicles issuing localization requests through CVL, optimizing communication energy consumption is crucial for reducing overall energy usage.
- **Computation**: In CVL, performing feature extraction and feature matching on high-resolution images incurs substantial computational resource consumption. However, the computing capabilities of UAVs and vehicles are limited, and excessive computational loads can lead to rapid battery depletion and increased device overheating. Moreover, feature extraction in CVL increasingly involves

multi-modal feature fusion, which further increases computational complexity. Although split-inference can alleviate the computational burden on terminal devices, optimization of computing strategies is still required to support concurrent multitasking on these devices.

- **Confidentiality**: In the 6G era, CVL systems will collect and transmit terabytes of visual data, and directly uploading raw images would pose significant risks to user privacy, commercial confidentiality, and national security. If all raw images are transmitted to the cloud, large-scale privacy data could be compromised through potential cloud-based attacks. The split-inference framework can avoid directly uploading raw data, yet original data can still be partially reconstructed through open-box or closed-box attacks. Therefore, optimizing the confidentiality of CVL is also essential.

The above analysis highlights the necessity of optimizing Tri-Co. However, optimizing a single dimension in isolation is insufficient; a joint optimization of Tri-Co is required. In particular, within the CVL architecture based on split-inference, the selection of partition points directly affects Tri-Co. When the model partition point is placed deeper, the UAV or vehicle extracts higher-dimensional image features, and the size of the intermediate features tends to decrease. This can

TABLE II: Matching Performance for Different Numbers of UAV-view and Ground-view Images (%).

(a) Limited number of ground-view images										
UAV↔Ground	1 vehicle-view image					2 vehicle-view images				
	Recall@1	Recall@5	Recall@10	Recall@top1	AP	Recall@1	Recall@5	Recall@10	Recall@top1	AP
1 UAV-view image	47.08	72.04	80.88	81.74	52.91	51.21	75.89	83.74	84.02	56.76
2 UAV-view images	48.36	72.75	81.31	82.03	54.02	51.36	76.89	84.59	85.16	57.06
3 UAV-view images	47.65	73.18	81.60	82.88	53.40	51.64	77.89	84.45	85.59	57.49
4 UAV-view images	48.36	73.89	82.45	83.59	54.09	52.21	78.46	85.45	85.88	58.11

(b) Increasing the number of ground-view images										
UAV↔Ground	3 vehicle-view images					4 vehicle-view images				
	Recall@1	Recall@5	Recall@10	Recall@top1	AP	Recall@1	Recall@5	Recall@10	Recall@top1	AP
1 UAV-view image	53.64	77.46	83.74	84.17	59.07	54.21	78.03	84.59	84.88	59.61
2 UAV-view images	53.64	77.89	85.02	86.16	59.21	55.06	78.74	85.16	86.45	60.40
3 UAV-view images	54.78	78.82	86.86	87.02	60.17	56.09	79.03	85.88	86.45	61.26
4 UAV-view images	55.63	79.74	85.88	86.88	60.95	55.92	79.89	86.31	86.88	61.35

reduce the communication energy consumption and latency of terminal devices, and also enhance the confidentiality of raw data, but the computational energy consumption increases. When the model partition point is placed earlier, the UAV or vehicle extracts lower-dimensional image features, and the size of the intermediate features tends to increase. This results in increased communication energy consumption and latency on terminal devices, reduced confidentiality of raw data, and lower computational energy consumption.

Part (b) of Fig. 2 illustrates the QoS optimization scheme based on reinforcement learning, which performs the joint optimization of Tri-Co. First, the state of the 6G SAGIN is recorded, including channel parameters, device battery status, computing resource availability, and other environmental information relevant to CVL. Subsequently, the configurations of the feature extraction models in CVL are recorded, including the model partition points used by UAVs and vehicles. Since UAVs and vehicles differ in computing capabilities, battery capacities, and other parameters, the selected model partition points may vary accordingly. The overall optimization objective of the system is to minimize communication, computation, and confidentiality costs. Accordingly, the system's reward function can be defined as the weighted sum of these three costs, and maximizing the additive inverse of this sum achieves the maximization of the system reward. Fig. 2 illustrates an off-policy deep reinforcement learning network, where experience replay is employed to maximize sample utilization and improve training stability. The Critic network outputs evaluations of actions, while the Actor network generates model partitioning strategies and applies them to CVL. The joint optimization of Tri-Co is not limited to off-policy reinforcement learning methods. We can adopt policy-based reinforcement learning or other optimization approaches depending on practical requirements [14].

IV. CASE STUDY

This section evaluates the performance of CVL based on 6G SAGIN and analyses as well as optimizes communication, computation, and confidentiality within the split-inference

framework. The related experimental code is available in the footer link. ¹

A. Experimental Configurations

In the case study, three experiments are designed as follows:

- **Experiment 1:** The feasibility and localization performance of UAVs or vehicles using CVL based on 6G SAGIN are evaluated through simulation experiments. The experiment is configured with varying numbers and viewpoints of images for matching.
- **Experiment 2:** By simulating open-box and closed-box attacks, the effectiveness of protecting raw data at different model partition points in split-inference is evaluated. The experiment conducts a quantitative evaluation of the reconstructed images.
- **Experiment 3:** A mathematical model is established for the joint optimization of communication, computation, and privacy in the QoS metrics of CVL. The formulated optimization problem is solved using a range of reinforcement learning algorithms, and the convergence performance of different algorithms is compared.

Specifically, in Experiment 1, we adopt ResNet-50 as the backbone feature extraction model, with two uncertainty-aware spatial attention modules (USAMs) incorporated to enhance feature matching performance. UAV or vehicle images often suffer from noise, viewpoint variations, and occlusions. USAM incorporates uncertainty information to dynamically adjust the attention distribution, thereby enhancing the robustness of feature selection. We insert the two USAM modules after the Stem and after Stage 1 of ResNet-50, respectively. The simulation scenarios cover localization for both UAVs and vehicles. For UAV localization, we use satellite-view and vehicle-view images as reference images, whereas for vehicle localization, satellite-view and UAV-view images serve as the references. The dataset used is University-1652, which contains satellite, UAV, and vehicle-view images of 1,652

¹https://github.com/xuyanbing11/cross_view_file/tree/main

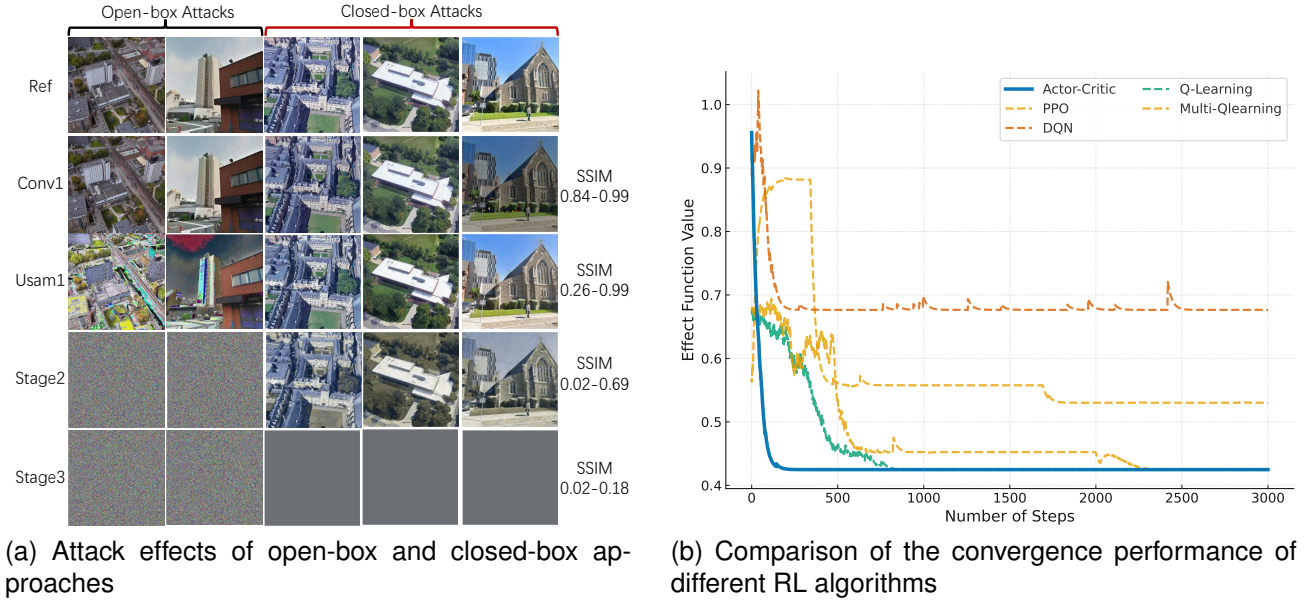


Fig. 3: Data security of CVL with split-inference and the joint optimization performance of Tri-Co.

buildings from 72 universities [15]. In the experiments of this work, one satellite image, four UAV images, and four vehicle-view images were selected for each building, and the impact of varying image quantities on localization accuracy was investigated. We employ Recall@K and average precision (AP) to evaluate the effectiveness of feature matching, thereby assessing the performance of CVL. We use Recall@K to measure whether the system successfully retrieves the correct matching image within the top-K results. If the true matching building image appears among the top K retrieved results, the Recall@K is set to 1; otherwise, it is 0. Since Recall@K cannot handle multiple matches, we also adopt AP in the experiments to provide a more comprehensive evaluation of localization performance. The AP is calculated by averaging the precision values at the ranks where each true matching image appears. A higher AP indicates that more true matches are retrieved earlier, reflecting better localization performance.

In Experiment 2, open-box and closed-box attacks are carried out on models with different partition points. The open-box attack refers to a scenario in which the attacker has full knowledge of the target model, including its architecture, parameter weights, and gradient information, and exploits this knowledge to infer the original data, thereby causing privacy leakage. The closed-box attack refers to a scenario in which the attacker only has access to intermediate features and the distribution of the original data, and attempts to steal privacy information by training an inversion model to reconstruct the original data. We select model partitioning at the convolutional layer of the improved ResNet-50 network, after the first USAM module, Stage 2, Stage 3, and Stage 4. We apply this partitioning strategy identically to both UAVs and vehicles. To evaluate the difference between the reconstructed images from the two types of attacks and the original images, we use the structural similarity index (SSIM) for quantitative evaluation. The SSIM focuses on structural

information by jointly considering luminance, contrast, and structural similarity. Its value ranges from 0 to 1, with values closer to 1 indicating higher similarity between two images, and thus greater exposure of privacy information.

In Experiment 3, we use the NVIDIA Quadro P400 to simulate the computing platform of a UAV. It provides a peak FP32 performance of 0.641 TFLOPS with a maximum power consumption of 30W. Its single-slot design and ultra-low power consumption make it well-suited for lightweight professional graphics and computing tasks. We then use the NVIDIA DRIVE AGX Xavier to simulate the computing platform of a vehicle. Its GPU delivers 1.3 TFLOPS of single-precision (FP32) performance. The wireless communication cost between UAVs or vehicles and ground servers primarily considers latency and energy consumption, and it is mathematically described using Shannon’s formula. The selection of model partition points directly affects the size of the intermediate features to be transmitted. By performing a forward pass at the split point and examining the shape of the output tensor at that layer, the dimensions and size of the intermediate features can be determined, thereby enabling the calculation of the latency and energy consumption required for wireless communication with a ground server. The computational cost primarily considers the energy consumption of UAVs or vehicles during split-inference. Different choices of model partition points result in varying computational workloads on the terminal devices (UAVs or vehicles), thereby leading to differences in energy consumption. Based on the power consumption of floating-point operations for different devices, the corresponding computational energy consumption can be obtained. The cost of confidentiality is primarily evaluated based on open-box and closed-box attacks. We employ Kullback–Leibler (KL) divergence to measure the difference between the images generated by these attack models and the original images, with larger KL values indicating stronger

confidentiality. We use a weighted average of the ratios between the KL divergence obtained from open-box and closed-box reconstructions and the maximum KL divergence as the confidentiality cost value. The selection of partition points in the feature extraction model directly influences the quality of images reconstructed by open-box and closed-box attack models, thereby affecting the confidentiality of the original data.

After obtaining the three cost functions of communication, computation, and confidentiality for the CVL system, we formulate the optimization problem. The selection of partition points in the feature extraction model simultaneously affects the three costs mentioned above. Therefore, partition point selection can be treated as the optimization variable, with the minimization of the weighted sum of the three cost values serving as the optimization objective for the CVL system. Several fundamental reinforcement learning algorithms are applied to optimize the above problem, providing references for future research. The main algorithms include Actor-Critic, Q-Learning, Multi-Q-Learning, DQN, and PPO, all of which can serve as baselines for comparison with other algorithms.

B. Performance Analysis

Table II presents the matching performance between UAV-view and vehicle-view images under different settings. The results indicate that performance improves consistently as the number of UAV-view and vehicle-view images increases. In the limited ground-view scenario, adding more UAV-view images enhances recall and AP, with the best performance observed when four UAV-view images are combined with two vehicle-view images. When the number of ground-view images is further increased, the improvement becomes more significant, and the highest accuracy is achieved with four UAV-view and four vehicle-view images (Recall@top1 = 86.88%, AP = 61.35%). These findings highlight the critical role of multi-view integration in enhancing cross-view matching accuracy and robustness. These findings also demonstrate that CVL based on 6G SAGIN offers broad opportunities for further research. For example, future work should examine how to select from the massive volume of images provided by 6G SAGIN to improve CVL accuracy, and how to integrate multi-view images to enhance CVL efficiency.

Fig. 3a demonstrates the attack effects of open-box and closed-box approaches at different feature extraction stages. The first row presents the original images as a reference, while the subsequent four rows display the reconstruction results of the two attack approaches under different partition points in split-inference. Under open-box attacks, the difficulty of reconstructing the original images increases as the model partition point becomes deeper, resulting in images at Stage 2 and Stage 3 being almost completely corrupted and visually unrecognizable. In contrast, closed-box attacks preserve more structural content, but image fidelity still degrades progressively with increasing depth. The SSIM values on the right-hand side quantitatively confirm this trend: while shallow partition points (Conv1) maintain relatively high similarity scores (0.84–0.99), deeper partition points cause the similarity

to drop sharply, reaching as low as 0.02–0.18 at Stage 3. Fig. 3a does not present the reconstruction results for the partition point at Stage 4, as the images can no longer be recovered at this stage. These results demonstrate that as the partition point moves deeper into the neural network, the confidentiality of the original data becomes stronger. Naturally, the communication and computation resources also change accordingly.

Fig. 3b compares the convergence performance of different reinforcement learning algorithms in terms of effect function value over training steps. The horizontal axis represents 3,000 sampled training steps, while the vertical axis denotes the effect function value, defined as the weighted sum of communication, computation, and confidentiality costs. The results show that the Actor-Critic method achieves the fastest and most stable convergence, reaching a lower effect function value of around 0.42 with minimal fluctuations. Q-Learning also converges but exhibits slower reduction and greater variability in effect function value. In contrast, DQN, PPO, and Multi-Q-learning demonstrate unstable convergence behaviour and remain at higher function values, indicating inferior optimization performance. Overall, Actor-Critic consistently outperforms the other methods, highlighting its superiority in achieving both rapid convergence and stability in this scenario.

V. FUTURE DIRECTIONS

A. Multi-Source Visual Fusion and Cross-Modal Feature Alignment

Future research is expected to develop advanced strategies for multi-source visual fusion and cross-modal feature alignment. By harmonizing heterogeneous imagery across space, air, and ground views, feature representations can be unified to improve CVL. Lightweight fusion models and self-supervised adaptation will enhance robustness against modality gaps, enabling scalable and reliable localization systems.

B. Ultra-Low-Latency Visual Data Collaboration based on 6G SAGIN

Leveraging 6G SAGIN, future studies are anticipated to focus on ultra-low-latency visual data collaboration. Adaptive task offloading and cross-layer optimization will reduce end-to-end delays, while balancing communication, computation, and energy cost. Such efforts will support seamless UAV–vehicle cooperation, ensuring real-time performance in dynamic and resource-constrained environments.

C. Privacy-Preserving and Secure Trusted Localization

Ensuring privacy-preserving and secure trusted localization is critical for practical deployment. Future research can integrate cryptographic primitives, distributed learning, and verifiable computation frameworks. These approaches will protect sensitive visual data, enhance system accountability, and strengthen resilience against adversarial attacks, while maintaining localization accuracy in diverse mission-critical scenarios.

D. Digital Twins and Multi-Dimensional Intelligent Interaction

The integration of digital twins will enable multi-dimensional intelligent interaction in CVL. High-fidelity virtual replicas of physical environments can support real-time visualization, predictive analytics, and collaborative decision-making. Embedding adaptive feedback loops will expand applications in smart cities, disaster response, and autonomous navigation, enhancing situational awareness and operational efficiency.

E. Agentic AI-Driven Cross-View Localization in 6G SAGIN

Future work is anticipated to harness Agentic AI to enable autonomous and adaptive CVL in 6G SAGIN. By combining multi-agent reinforcement learning, semantic communication, and memory-augmented coordination, distributed agents can achieve intelligent cooperation. This paradigm will improve robustness, scalability, and autonomy, paving the way for next-generation localization services.

VI. CONCLUSION

In this paper, we have investigated efficient CVL based on SAGIN, focusing on how CVL can be integrated with the 6G network architecture. First, we have provided an overview of CVL and 6G SAGIN. We have conducted a comparison between single-view and cross-view image localization. We have also summarized the fundamental methods and potential applications of CVL, and illustrated the importance of CVL based on 6G SAGIN through an example of UAV flight in an urban canyon. Subsequently, we have proposed a split-inference-based CVL framework within the 6G SAGIN architecture. We have designed this framework to enhance the efficiency and accuracy of cross-domain visual localization for low-altitude and ground devices by integrating the communication and computation resources of space-air-ground elements within the 6G network. Moreover, we have analyzed the impact of feature extraction model partition points on the user experience of CVL within the proposed framework, and have introduced a reinforcement learning-based joint optimization method for communication, computation, and confidentiality. In the case study, we have verified the proposed split-inference framework and joint optimization method. The experimental results have shown that the framework improves localization accuracy, while the performance of CVL in latency, energy consumption, and privacy protection is jointly optimized in a balanced manner. Finally, we have discussed potential directions for future research.

REFERENCES

- [1] L. P. Qian, X. Fan, M. Li, and Y. Wu, "Energy-Efficient Data Gathering and Computing in LEO Satellite-assisted Marine IoT Networks," *IEEE Transactions on Cognitive Communications and Networking*, pp. 1–1, Aug. 2025.
- [2] Q. Wu, Y. Wan, Z. Zheng, Y. Zhang, G. Wang, and Z. Zhao, "CAMP: A Cross-View Geo-Localization Method Using Contrastive Attributes Mining and Position-Aware Partitioning," *IEEE Transactions on Geoscience and Remote Sensing*, vol. 62, pp. 1–14, Aug. 2024.

- [3] K. Wang, X. Wang, N. Zhao, X. Yang, H. Fang, and D. Niyato, "Uplink RSMA in LEO Satellite Communications: A Perspective From Generative Artificial Intelligence," *IEEE Transactions on Vehicular Technology*, pp. 1–6, Jun. 2025.
- [4] J. Du, H. Wang, C. Jiang, J. Simonjan, J. Wang, and M. Debbah, "Distributed AI-Based Secure Communications in Space-Air-Ground-Sea Integrated Networks," *IEEE Communications Magazine*, vol. 63, no. 7, pp. 48–55, Jun. 2025.
- [5] C. Chen, B. Wang, C. X. Lu, N. Trigoni, and A. Markham, "Deep Learning for Visual Localization and Mapping: A Survey," *IEEE Transactions on Neural Networks and Learning Systems*, vol. 35, no. 12, pp. 17 000–17 020, Sep. 2024.
- [6] K. Xie, W. Zhou, X. Huang, H. Guan, and F. Yulong, "Self-Supervised Cross-View Graph Search Framework for Ground-to-Satellite Geo-Localization," *IEEE Transactions on Geoscience and Remote Sensing*, vol. 63, pp. 1–14, Aug. 2025.
- [7] K. Wang, S. Luo, T. Chen, and J. Lu, "Salient-VPR: Salient Weighted Global Descriptor for Visual Place Recognition," *IEEE Transactions on Instrumentation and Measurement*, vol. 71, pp. 1–8, Nov. 2022.
- [8] Y. Gao, H. Liu, and X. Wei, "Semantic Concept Perception Network With Interactive Prompting for Cross-View Image Geo-Localization," *IEEE Transactions on Circuits and Systems for Video Technology*, vol. 35, no. 6, pp. 5343–5354, Jan. 2025.
- [9] X. Zhou, X. Yang, and Y. Zhang, "CDM-Net: A Framework for Cross-View Geo-Localization With Multimodal Data," *IEEE Transactions on Geoscience and Remote Sensing*, vol. 63, pp. 1–16, Jul. 2025.
- [10] S. Mahboob and L. Liu, "Revolutionizing Future Connectivity: A Contemporary Survey on AI-Empowered Satellite-Based Non-Terrestrial Networks in 6G," *IEEE Communications Surveys & Tutorials*, vol. 26, no. 2, pp. 1279–1321, Jan. 2024.
- [11] Y. Xiao, Z. Ye, M. Wu, H. Li, M. Xiao, M.-S. Alouini, A. Al-Hourani, and S. Cioni, "Space-Air-Ground Integrated Wireless Networks for 6G: Basics, Key Technologies, and Future Trends," *IEEE Journal on Selected Areas in Communications*, vol. 42, no. 12, pp. 3327–3354, Nov. 2024.
- [12] J. Tan, F. Tang, M. Zhao, and N. Kato, "Outage Probability, Performance, and Fairness Analysis of Space–Air–Ground Integrated Network (SAGIN): UAV Altitude and Position Angle," *IEEE Transactions on Wireless Communications*, vol. 24, no. 2, pp. 940–954, Nov. 2025.
- [13] J. Wang, G. Feng, Y.-J. Liu, X. Xu, L. Cheng, W. Jiang, and L. P. Qian, "Split Learning Based Cloud-Edge-End Collaborative Model Training in Heterogeneous Networks," *IEEE Transactions on Network Science and Engineering*, pp. 1–17, Aug. 2025.
- [14] C. Shang, J. Yu, and D. T. Hoang, "Energy-Efficient and Intelligent ISAC in V2X Networks with Spiking Neural Networks-Driven DRL," *IEEE Transactions on Wireless Communications*, pp. 1–1, Jul. 2025.
- [15] Z. Zheng, Y. Wei, and Y. Yang, "University-1652: A Multi-view Multi-source Benchmark for Drone-based Geo-localization," in *Proceedings of the 28th ACM international conference on Multimedia*, ser. MM '20, New York, NY, USA, Oct. 2020, p. 1395–1403.